

Crystallographic and Orientation Features of Nanocrystals in Thin Film Condensates PbTe-Bi₂Te₃ on Glass Ceramics

Ya.P. Saliy¹, D.M. Freik¹, I.S. Bylina¹, M.O. Galushchak²

¹ *Physical-Chemical Institute, Vasyl Stefanyk PreCarpathian National University, 57, Shevchenko Str., 76018 Ivano-Frankivsk, Ukraine*

² *Ivano-Frankivsk National Technical University of Oil and Gas, 15, Karpatska Str., 76019 Ivano-Frankivsk, Ukraine*

(Received 27 March 2015; revised manuscript received 20 April 2015; published online 10 June 2015)

With the help of the AFM-images analysis, using the discrete Fourier transformation, the autocorrelation function for the azimuthal angle φ and the amount of normal distributions for the polar angle ρ we have investigated the orientation process of structure formation of the nanocrystals in vapor-phase condensates of PbTe-Bi₂Te₃ solid solution on glass ceramics. It was detected that the substrate of glass ceramics does not depend on a particular orientation of crystallites. We determined that objects, which had been created by the planes of the cube, rhombic dodecahedron and their combinations, are formed on the sample surface. It was demonstrated the dependence between the average sizes of nanocrystals, their growth rate and the deposition time. We established the character of the dependence of the density distribution of the polar angle ρ and the Bi₂Te₃ content and duration of deposition.

Keywords: Lead telluride, Vapor-phase condensates, Nanocrystals, Symmetry, Crystallographic form.

PACS numbers: 64.60.Qj, 68.03.Fg

1. INTRODUCTION

Due to their unique properties, nanosized materials occupy a leading position in modern materials science. The development of science and technology is closely connected with the improvement of the existing and elaboration of new methods of obtaining and study of the nanosized structures. Quantum-size effects, which create completely new opportunities for application of the given materials in different fields of science and engineering, take place with the transition to the nanostructured materials [1].

Multi-component solid solutions allowing to vary in a rather wide range the material parameters find more applications in the production of new semiconductor devices. In particular, solid solutions based on lead telluride have proved to be important industrial materials, which can be widely used in thermoelectricity [2-4]. We should note that PbTe is an efficient thermoelectric material in the medium-temperature region of (500-750) K [2, 5], and solid solutions on its basis allow to obtain a material with improved parameters necessary for the production of thermoelectric units.

As for the thin-film condensate of PbTe-Bi₂Te₃ solid solution, it opens new possibilities of its practical application conditioned by the features of formation of separate nanostructures [6].

In order to obtain thin-film condensates, the vapor-phase vacuum technologies are widely used [2-7]. The morphological changes of the surface of built up layers on account of the mechanical stresses conditioned by the mismatch in the lattice constants, linear expansion coefficients of condensates and substrates, on which they are deposited, occur in their implementation.

Development of the atomic force microscopy (AFM) and other methods of high resolution opens new opportunities for observation and analysis of the growth stages and formation of nano-objects of different sizes. Study of the orientation and structural features of formation of na-

nocrystals on the surface of thin films is an important step in the development of modern thin-film materials science.

Therefore, in this work, which is a logical extension of the previous investigations [8, 9], based on the analysis of the AFM-images we present the results of the study of the statistical regularities in the processes of the orientation structure-formation of nanocrystals in vapor-phase PbTe-Bi₂Te₃ condensates on glass ceramic substrates.

2. MATERIALS AND METHODS OF STUDY

PbTe-Bi₂Te₃ condensates are obtained by the method of open evaporation in vacuum. Plates of polycrystalline glass ceramics, which were chemically pre-cleaned, were used as the substrates. Pre-synthesized solid solution PbTe-Bi₂Te₃, in which content of Bi₂Te₃ was varied in the range of (1-5) mol. %, served as the material for deposition. Evaporation temperature T_E was equal to 970 K, and deposition temperature T_S was 470 K. Deposition duration τ was varied within (15-75) s. Thickness of the obtained condensate was measured using microinterferometer MII-4.

The surface topology of the samples was determined by the AFM-method Nanoscope 3a Dimension 3000 (Digital Instruments, USA) in the periodic contact mode. The measurements are performed in the central part of the samples using serial silicon probes NSG-11 with the nominal rounding radius of the point to 10 nm. Square field of the condensate of size of 1 μm^2 is represented by the array of 512² points.

By the results of the AFM-investigations in the environment of Gwyddion software, we have determined the average sizes of nanostructures in the normal h_c and lateral D_c to the substrate surface directions (Table 1). Based on the obtained results, we have plotted the dependences of these characteristics and the rate of their change on the deposition duration.

We have also determined the averaged polar ρ and azimuthal φ angles for all points of the condensates sur-

faces. The obtained experimental results were analyzed by using the discrete Fourier transformation $F(k)$ of the function $f(n)$ according to

$$F(k) = \sum f(n) \exp(-in2\pi k / N) \quad (1)$$

and the autocorrelation function $C(l)$

$$C(l) = (\sum f(l+n)f(n) / N)^{1/2} \quad (2)$$

of the distribution of the azimuthal angle φ of nano-objects in accordance with [8, 9].

The values of the polar angles ρ were approximated by the sum of two normal distributions

$$f(\rho) = A_1 \exp(-(\rho - \rho_{m1})^2 / \sigma_1^2) / (2\pi \sigma_1^2)^{1/2} + A_2 \exp(-(\rho - \rho_{m2})^2 / \sigma_2^2) / (2\pi \sigma_2^2)^{1/2}. \quad (3)$$

Phase composition of the synthesized $\text{PbTe-Bi}_2\text{Te}_3$ solid solution was determined by the X-ray radiography on the device DRON-3 by the powder method in chrome radiation in the Bragg-Brentano geometry in the range of scan angles $20^\circ \leq 2\theta \leq 110^\circ$. Processing of the results of the X-ray phase analysis was carried out by the method of Rietveld refinement using the FulProf program package. The studied samples, which passed through different stages of preparation and processing, were found to be almost equal. $\text{Pb}_{1-x}\text{Bi}_x\text{Te}$ of the NaCl structural type can be considered the main phase (Fm-3m space group) with the parameter of the unit face-centered cubic cell of $a = 6.4564$.

3. EXPERIMENTAL RESULTS AND DISCUSSION

Some of the results of the AFM-study of the surface of $\text{PbTe-Bi}_2\text{Te}_3$ condensates deposited on the substrates of glass ceramics are illustrated in Fig. 1 and Fig. 2 and represented in Table 1. We should note that the main feature of glass ceramics is the fact that this material contains a great amount of fine ($< 1 \mu\text{m}$) crystallites connected by a glassy intercrystalline interlayer; therefore, epitaxial objects on its surface can be formed on separate planes of crystallites. Pores, cavities and other defects are absent, as a rule, in the bulk of this material, and its good heat resistance (linear extension coefficient $\alpha \approx (5-10) \cdot 10^{-7} \text{ 1/K}$) and rather high heat conduc-

tivity (2.1-5.5 W/m·K) make the material interesting for application as the substrate in the study of the growth features of epitaxial vapor-phase structures. The process parameters play no less important role during deposition, since they determine the processes of nucleation, growth and formation of separate dome-shaped islands on the condensate surface.

Thus, the processes which include nucleation of a new phase in the form of separate dome-shaped islet nano-formations of the height of (10-45) nm and diameter of (30-65) nm (Fig. 1a; Table 1) take place for the studied samples on the initial deposition stages at the optimized values of the evaporation ($T_E = 970 \text{ K}$) and substrate ($T_S = 470 \text{ K}$) temperatures. Then, nucleation of new islets ceases, and molecules adsorbed on the surface participate in the growth of the already formed structures.

On the late deposition stages ($\tau = 60-75 \text{ s}$) the coalescence mode is realized, at which merging of individual nanostructures occurs that conditions the decrease in their density and increase in the normal and lateral sizes resulting in the increase in the surface roughness (Fig. 1c, Table 1).

We should note that with increasing total thickness d of the condensates (Table 1, Fig. 2a, curve 1, \blacktriangle) with deposition time τ , the average normal h_c and lateral D_c sizes of nanocrystals have a tendency to saturation (see Fig. 2a, curves 2, \blacksquare ; 3, \bullet), and their growth rates $h/d\tau$ and $D/d\tau$ decrease (Fig. 2b, curves 2, \blacksquare ; 3, \bullet). This effect is explained by the fact that with increasing deposition duration, the nanostructures become more massive and, correspondingly, each attachment of the same number of atoms or clusters to a certain islet will contribute a smaller share to the growth of the given nanostructure in the normal or lateral direction. At that, deposition rate d/τ is characterized by a certain minimum in the average time interval (Fig. 2b, curve 1, \blacktriangle).

The controlled growth of the thin-film structures with the necessary properties can be realized by the growth processes. Description of the real kinetics of formation of new phase nuclei and further filling of the deposited surface is one of the main problems of the theory of the first-order surface phase transitions. The authors of [10] study the kinetic growth model of a thin film on a solid substrate under the condition of two-dimensional nucleation.

Table 1 – Technological factors and the most probable values of the polar angle ρ_m of the bimodal distribution and coefficients of comparison of the contributions of different-shaped planes K_φ and K_ρ of nanostructures in the vapor-phase $\text{PbTe-Bi}_2\text{Te}_3$ condensates on glass ceramics

Sample No	Content of x , % Bi_2Te_3	τ^* , s	d^* , nm	$\rho_{m1} \pm \sigma_1$	$\rho_{m2} \pm \sigma_2$	K_ρ	K_φ
4	5	15	270	12 ± 6	22 ± 10	4.9	1.3
5		30	410	20 ± 10	36 ± 13	0.7	0.8
6		45	540	27 ± 12	50 ± 13	3.7	0.4
7		60	810	27 ± 4	50 ± 13	1.8	0.2
8		75	1220	21 ± 11	41 ± 12	0.1	1.6
16	3	15	160	11 ± 6	24 ± 13	2.7	1.0
15		30	270	9 ± 5	23 ± 16	0.7	3.2
14		60	1000	12 ± 10	33 ± 17	1.5	3.9
13		75	1220	23 ± 11	52 ± 10	4.2	0.4
24	1	15	410	14 ± 8	28 ± 13	0.4	1.0
23		30	630	9 ± 6	21 ± 12	0.7	1.2
22		60	920	12 ± 6	27 ± 14	1.3	1.4
21		75	2030	11 ± 6	38 ± 16	1.3	2.1

Notation: τ^* – deposition time; d^* – condensate thickness

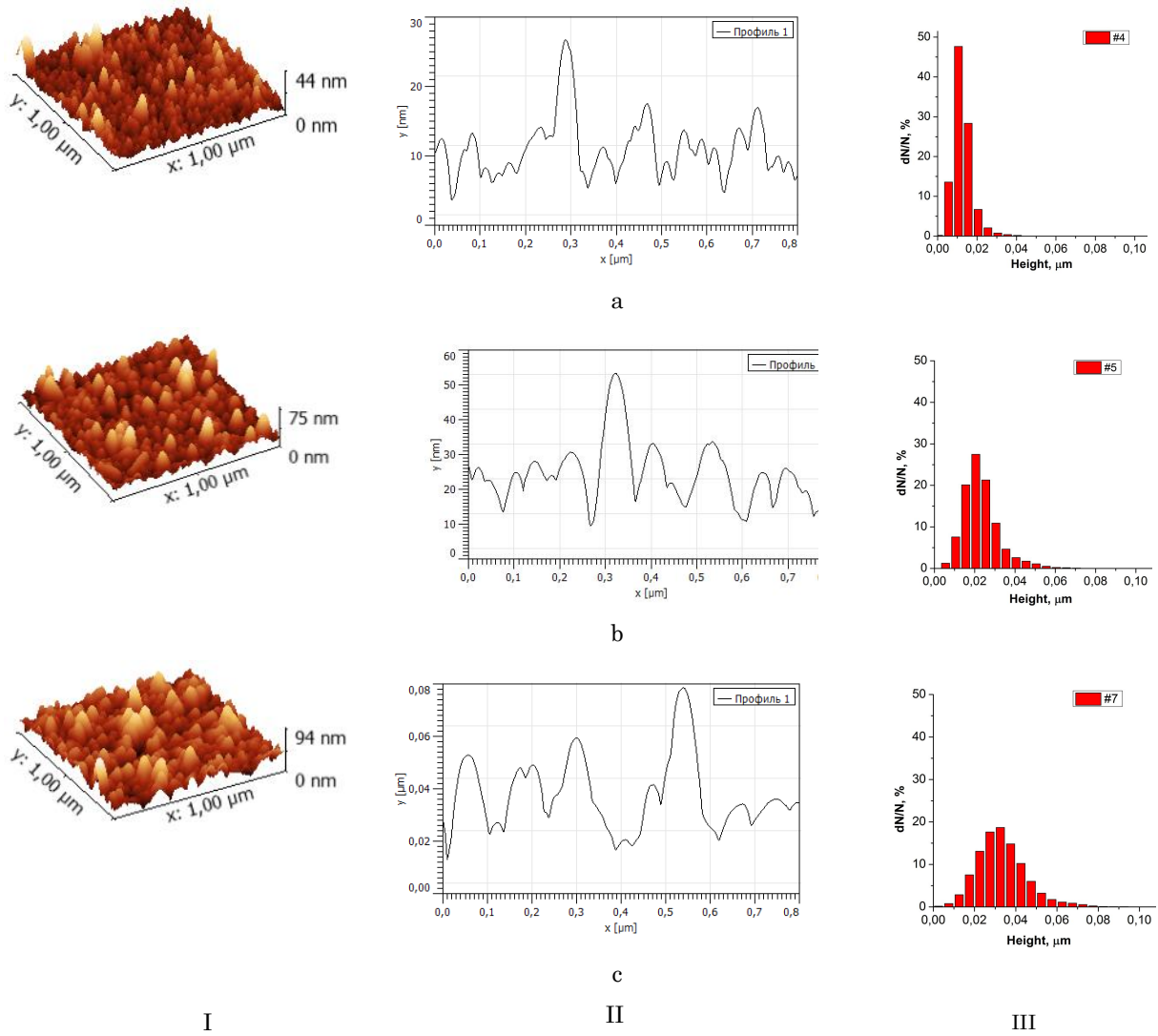


Fig. 1 – 3D AFM-images (I), profilograms (II) and histograms of the height distribution (III) of the surface of vapor-phase PbTe-5 mol. % Bi₂Te₃ condensates obtained on the substrates of glass ceramics for the deposition time τ , s: 15 (a, No4), 30 (b, No5) and 60 (c, No7); $T_E = 970$ K, $T_S = 470$ K

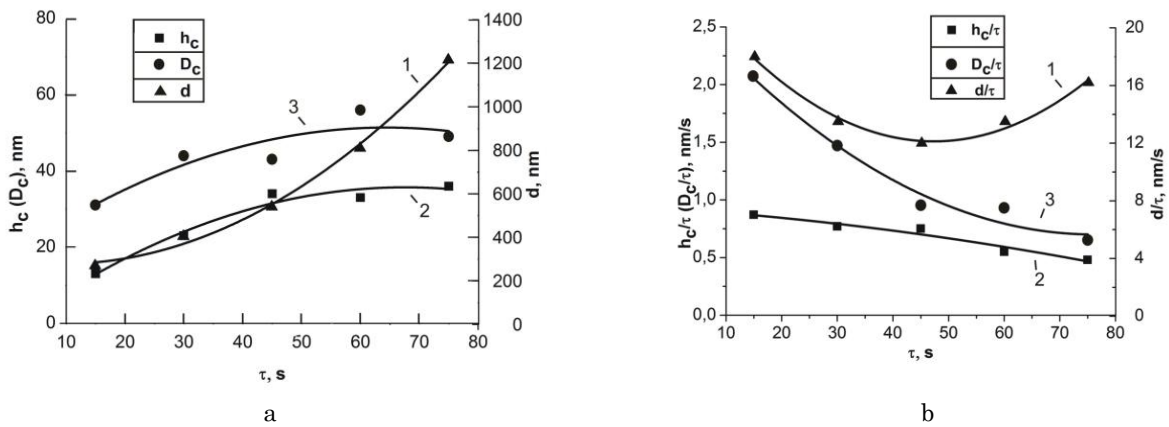


Fig. 2 – Dependences of the film thickness d (\blacktriangle , 1) and average normal h_c (\blacksquare , 2) and lateral D_c (\bullet , 3) sizes of nanocrystallites (a); their deposition d/τ (\blacktriangle , 1) and growth h_c/τ (\blacksquare , 2), D_c/τ (\bullet , 3) rates of vapor-phase PbTe-5 mol. % Bi₂Te₃ condensates on the substrates of glass ceramics on the deposition time τ , s; $T_E = 970$ K, $T_S = 470$ K

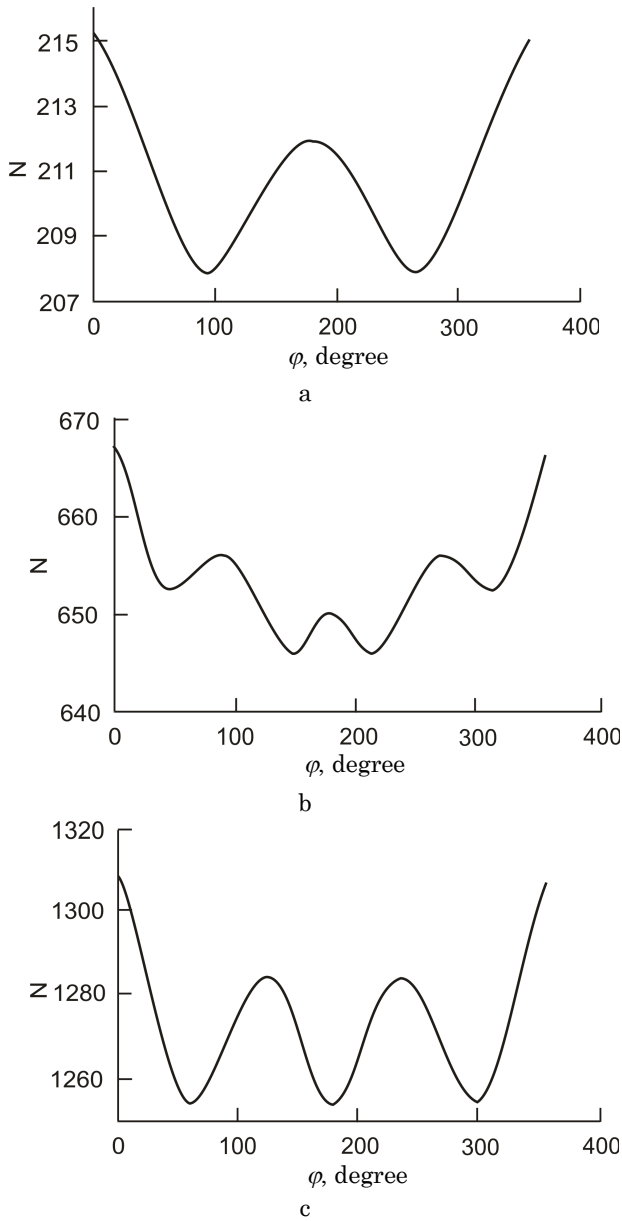


Fig. 3 – Typical autocorrelation distribution functions of the azimuthal angle φ of nanocrystals in vapor-phase condensates PbTe-5 mol. % Bi₂Te₃ on glass ceramics for deposition time τ , s: 15 (a, sample No4), 30 (b, No5), 45 (c, No6); Table 1

In conditions of a large supersaturation of the gas phase, they obtained the solutions for the distribution function of islets in sizes on the initial growth stage, substrate filling factor on the coalescence stage, vertical growth rate of the film and its surface roughness. In particular, the authors theoretically proved that after the beginning of nucleation, the following law takes place: the average islet size grows in proportion to deposition time as $\tau^{1/2}$.

In this connection, time dependences of the average normal h_c and lateral D_c sizes for the chosen set of samples (see Fig. 2a) were approximated in our study by the function of the form of $y = ax^b$, where $y = h_c, D_c$; a is a proportionality factor ($a = h_0, D_0$); $x = \tau$; b is the exponent. As a result, we obtained the value of b for the average normal sizes h_c , which was equal to $b = 0.62 \pm 0.14$ and can be approximately considered as $b \approx 1/2$. For the average lateral sizes D_c $b = 0.44 \pm 0.08$, i.e. in this case

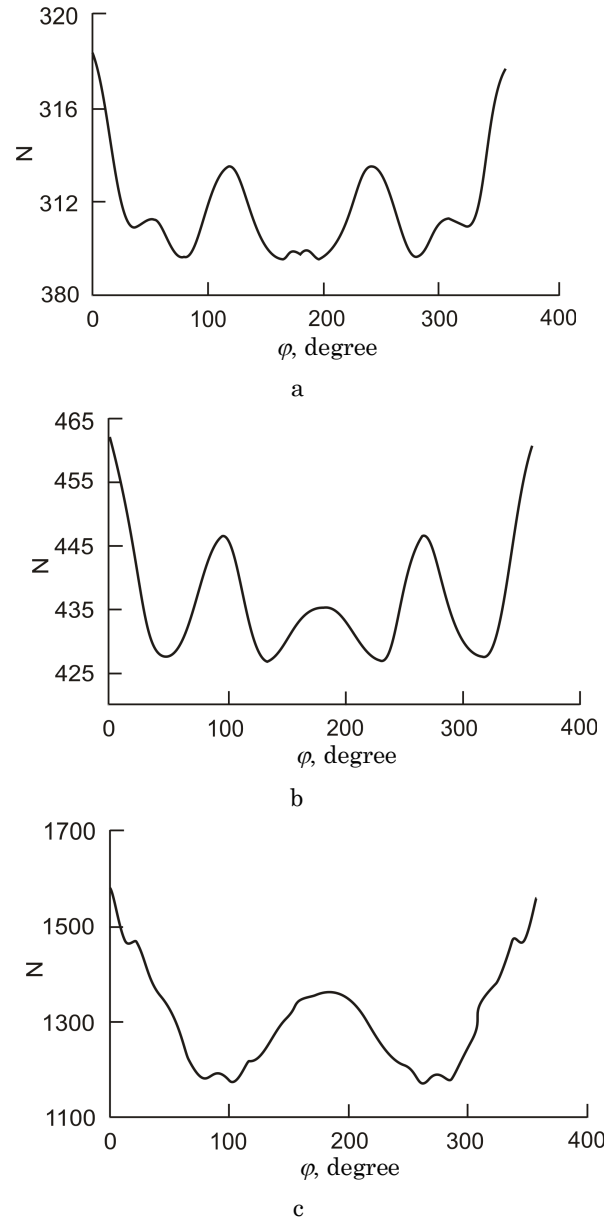


Fig. 4 – Typical autocorrelation distribution functions of the azimuthal angle φ of nanocrystals in vapor-phase condensates PbTe-3 mol. % Bi₂Te₃ on glass ceramics for deposition time τ , s: 15 (a, sample No16), 30 (b, No15), 60 (c, No14); Table 1

$b \approx 1/2$, too. So, the growth of the average normal h_c and lateral D_c sizes of PbTe-Bi₂Te₃ nanostructures is really proportional to $\tau^{1/2}$ that is confirmed experimentally.

The orientation features and crystallographic forms of nanocrystals in the vapor-phase condensates were determined by their averaged azimuthal φ and polar ρ angles in accordance with [8].

The discrete Fourier transformation (1) and the autocorrelation function (2) of the distribution of the azimuthal angle φ of surface elements of the samples AFM-images were used for the analysis.

In order to reveal the influence of the substrate on the orientation of the objects on the film surface, which can be represented by the orientation of the 3-d and 4-th order axes, we introduced the coefficient characterizing the ratio of the components amplitudes of the third and fourth harmonics of the Fourier transformation F_k :

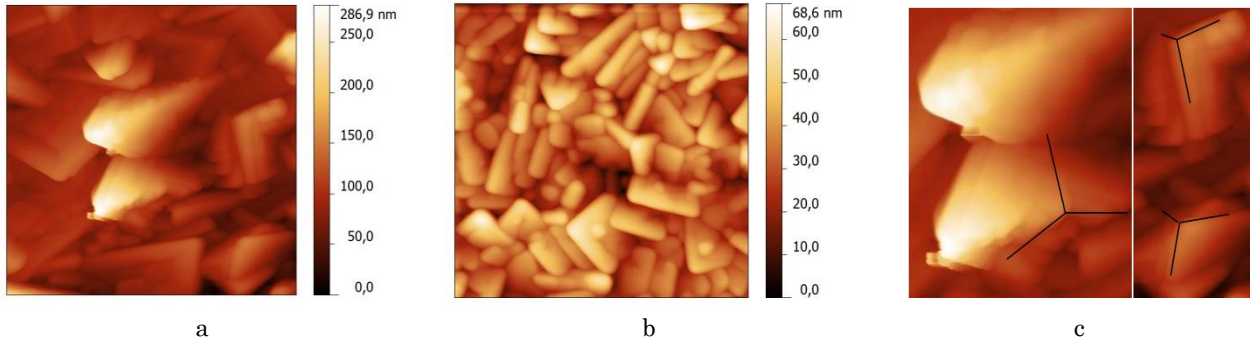


Fig 5 – AFM-images of the surface of PbTe-1 mol. % Bi₂Te₃ samples obtained at the deposition time $\tau = 75$ s (a, No21) and $\tau = 60$ s (b, No22) and also the scaled-up parts of them, on which the cube edges are depicted (c)

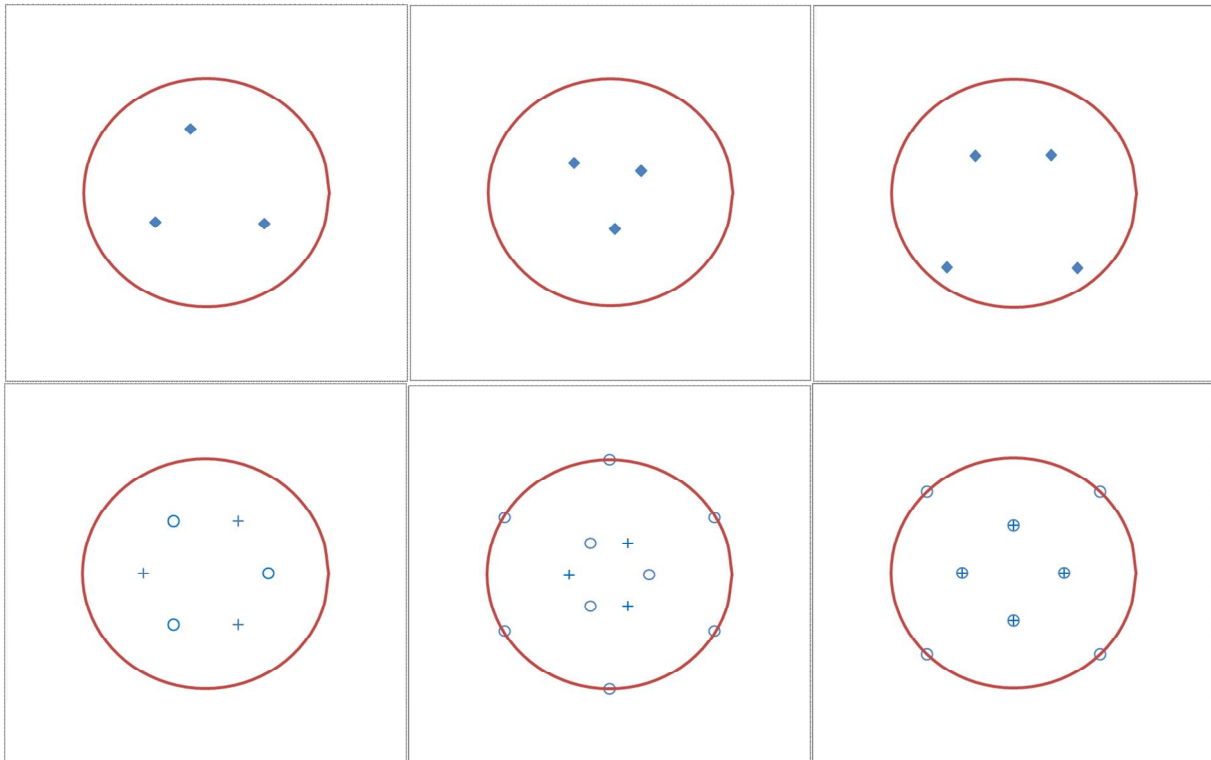


Fig. 6 – Gnome-stereographic projections of the objects on the films (No6, No7, No13) surface (the top row); cube and rhombic dodecahedron, if polar axis is directed along [111] and rhombic dodecahedron, if polar axis is directed along [001] (the low row). The objects are listed from left to right

$$K_{\varphi} = F_3 / F_4.$$

The values of this coefficient are given in Table 1.

With increasing deposition time for 5 mol. % Bi₂Te₃, the lateral symmetry is changed from the 2-nd (the 3-d order axis is present and weakly expressed) order (see Fig. 3a) firstly to the 4-th (the 3-d order axis is also exhibited) (Fig. 3b) and then to the 3-d (Fig. 3c) orders.

For deposition times of 60 s (sample No7) and 75 s (sample No8), the order of symmetry is changed again from the 3-d to the 4-th one (Table 1). We should note, if for small times $K_{\varphi} = 4.9$, then for large times this value decreases to $K_{\varphi} = 0.1$, i.e. it is possible to state that with increasing deposition time, contribution of the 3-d order axis relative to the contribution of the 4-th order axis sharply decreases.

With increasing deposition time for 3 mol. % Bi₂Te₃, the lateral symmetry is changed from the 3-d (to a lesser extent, 6-th) order (see Fig. 4a) firstly to the 4-th (3-d

(Fig. 4b), and then to 2-nd (3-d, 4-th) (Fig. 4c) orders. As for the ratio of the components amplitudes of the 3-d and 4-th harmonics of the Fourier transformation K_{φ} , then the contribution of figures symmetrical with respect to the 3-d order axis over the figures symmetrical with respect to the 4-th order axis is changed from $K_{\varphi} = 0.7$ (at $\tau = 30$ s) to $K_{\varphi} = 4.2$ (at $\tau = 75$ s), i.e. exceeds the 3-d order axis (Table 1).

For all deposition times at 1 mol. % Bi₂Te₃, the 2-nd order lateral symmetry is a dominant one, and the contributions of the 3-d, 4-th and 6-th order axes are commensurable, although at small deposition times the contribution of the 4-th order axis exceeds the contribution of the 3-d and 6-th order axes.

Thus, the axis perpendicular to the film surface is not clearly expressed, and hence it follows that glass ceramic substrate does not specify the chosen orientation to PbTe crystallites or specifies a free orientation. Increase in the Bi₂Te₃ content leads to the 3-d order axis dominance.

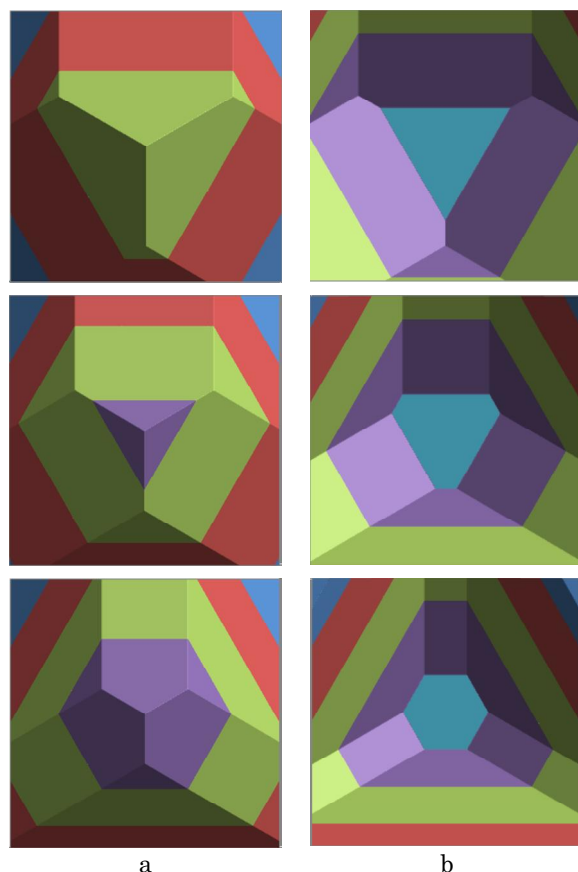


Fig. 7 – Compound form containing faces {100} and {110} (a), additionally depicted horizontal plane (111) (b). Contribution of swifter cube faces increases downwards

On all the samples except No21, on which twins are observed (Fig. 5), the 6-th order axis is not a dominant one, and the 3-d order axis is present everywhere that implies the formation of crystallites of the cubic system. Trigonal and tetragonal large pyramids as well as cube faces and edges are present in Fig. 5. Mismatch in the orientation of crystallites is manifested. The same situation was typical for the PbTe:Sb samples deposited on glass ceramics [8].

Now let us consider the individual objects in order to determine the simple crystallographic forms. To this end, we found orientation of their planes on the film surface. Triangular pyramids of the sample No6 are formed by the cube planes {100}, and of the sample No7 – by the rhombic dodecahedron planes {110}; at that plane (111) is parallel to the substrate. The object faces of the sample No13 correspond to the compound planes that combines cube and rhombic dodecahedron faces; here plane (001) is parallel to the substrate. The indicated above forms are shown in Fig. 6 using the gnomon-stereographic projections. Compound forms also with the pentagon-dodecahedron faces {120} are revealed on the surface of other films.

Different contributions of the faces of simple forms in the compound form are presented in Fig. 7, on which we show three cube faces (100), (010), (001) and three rhombic dodecahedron faces (110), (101), (011). Axis 6 is more clearly manifested with increasing contribution of the cube faces, and when contributions are commensurable, then axis 3 will prevail again.

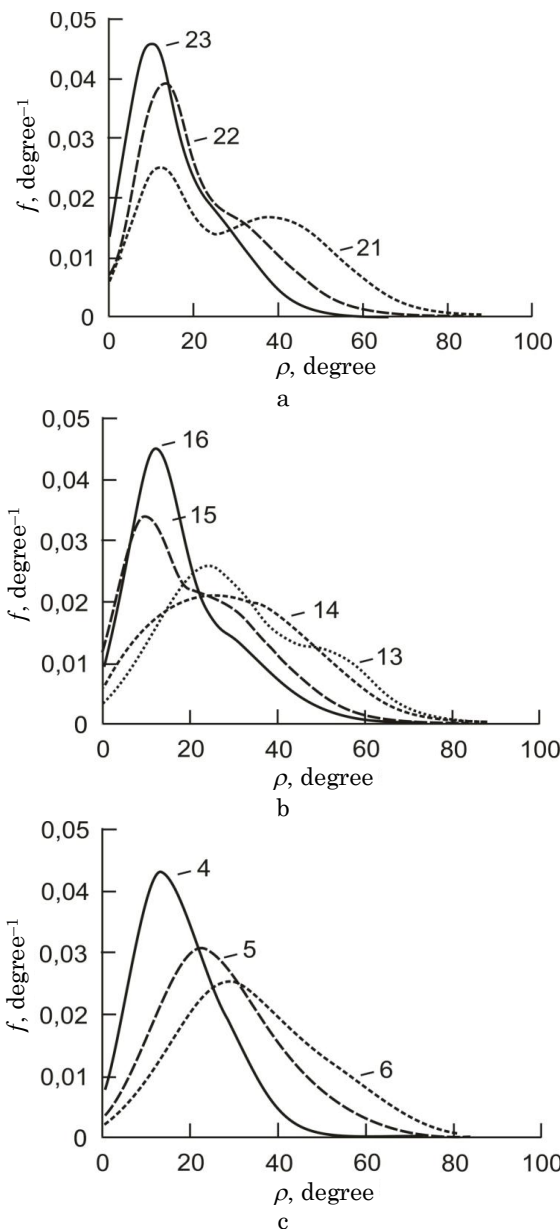


Fig. 8 – Dependence of the distribution density of polar angle ρ of nanocrystals in the vapor-phase PbTe-Bi₂Te₃ condensates on glass ceramics on the deposition time for Bi₂Te₃, mol. %: 1 (a), 3 (b), 5 (c); numbers near the curves correspond to the samples Table 1

Distribution density of the polar angle ρ was approximated by the sum of two normal distributions (3). In Table 1 we present the ratio of the right-to-left term amplitudes K_ρ . As seen from Table 1, polar angle of the dominant distribution is within the range of 20°-30°. 22.21° is the angle between the normal to the faces of the form {123} and direction [111]; this is the 3-d order axis in crystals of the cubic system. Swifter forms {110}, {120}, {100} appear with increasing content of Bi₂Te₃ and deposition time.

As seen from Fig. 8a, b, distribution has a bimodal nature. The dominant maximum is shifted towards larger angles with increasing deposition time. Presence of the peak at 22° is observed from both Table 1 and Fig. 8a. At doping by 5 mol. % Bi₂Te₃, bimodal distribution is not almost exhibited and both peaks merge into one (Fig. 8c).

4. CONCLUSIONS

1. Crystallographic forms of nanocrystals and their orientation features in thin-film condensates of PbTe-Bi₂Te₃ solid solutions grown on glass ceramic substrates by open evaporation in vacuum at the optimized evaporation $T_E = 970$ K and deposition $T_S = 470$ K temperatures are studied by the analysis of the AFM-images. Deposition time varied in the range of $\tau = 15-75$ s.

2. It is established that with increasing deposition time, average sizes of nano-objects in the normal h_c and lateral D_c to the substrate surface directions increase in proportion to $\tau^{1/2}$ and retain a tendency to saturation, and their growth rate decreases.

3. It is determined that glass ceramic substrate does not specify a certain orientation to crystallites; and the objects formed by the cube and rhombic dodecahedron

planes and their combinations are generated on the samples surface.

4. It is shown that at small content of Bi₂Te₃, distribution density of the polar angle ρ has a bimodal nature; at that, the dominant maximum is shifted towards larger angles with increasing deposition time. At 5 mol. % Bi₂Te₃, bimodal distribution is not almost exhibited, and both peaks merge into one.

ACKNOWLEDGEMENTS

The work has been performed within the research project of the Public Diplomacy Division of the NATO program "Science for Peace" (NUKR, SEPP 984536) and complex scientific project of the Ministry of Education and science of Ukraine (the state registration number 0115U002303).

REFERENCES

1. N. Kobayasy, *Vvedeniye v nanotekhnolohiyu* (M.: BYNOM. Laboratoriya znaniy: 2008).
2. D.M. Freik, M.A. Galushchak, L.I. Mezhilovskaya, *Fizika i tekhnologiya poluprovodnikovyykh plenok* (L'viv: Vishcha shkola: 1988).
3. L.P. Bulat, Ye.K. Iordanishvili, A.A. Pustovalov, M.I. Fedorov, *Termoelektrichestvo* 4, 7 (2009).
4. Z.M. Dashevskiy, *Termoelektrichestvo v khal'kogenidakh svintsa* (Gordon & Brich: 2002).
5. V.M. Shperun, D.M. Freik, R.I. Zapukhlyak, *Termoelektryka telurydu svyntsyu ta yoho analohiv* (Ivano-Frankivsk: Play: 2000).
6. S.P. Zymyn, E.S. Horlachev, *Nanostrukturirovaniye khalkohenidy svintsa* (Yaroslavl: YarHU: 2011).
7. Yu.Z. Bubnov, M.S. Lur'e, F.G. Staros, G.A. Filaretov, *Vakuumnoye nanoseniye plenok v kvaziamknutom ob'yeme* (Lvov: Energiya: 1975).
8. Ya.P. Saliy, D.M. Freik, I.S. Bylina, I.M. Freik, *Nanostrukturnoye materialovedeniye* No3-4, 20 (2013).
9. Ya.P. Saliy, I.I. Chaviak, I.S. Bylina, D.M. Freik, *J. Nano-Electron. Phys.* 6 No4, 04020 (2014).
10. V.G. Dubrovskiy, G.Ye. Tsyrlyn, *FTP* 39 No11, 1312 (2005).